

See discussions, stats, and author profiles for this publication at: <https://www.researchgate.net/publication/6209518>

Competition between DPPC and SDS at the air-aqueous interface

ARTICLE *in* LANGMUIR · SEPTEMBER 2007

Impact Factor: 4.46 · DOI: 10.1021/la7006974 · Source: PubMed

CITATIONS

24

READS

22

2 AUTHORS, INCLUDING:



Heather C Allen

The Ohio State University

126 PUBLICATIONS 3,389 CITATIONS

SEE PROFILE

Competition between DPPC and SDS at the Air–Aqueous Interface

Kandice L. Harper and Heather C. Allen*

Department of Chemistry, The Ohio State University, 100 West 18th Avenue, Columbus, Ohio 43210

Received March 9, 2007. In Final Form: May 29, 2007

Vibrational sum frequency generation spectroscopy is used to study the interactions of the charged soluble organic surfactant sodium dodecyl sulfate (SDS) with an insoluble 1,2-dipalmitoyl-*sn*-glycero-3-phosphocholine (DPPC) monolayer at the air–aqueous interface. Results indicate that the surfactant species compete for surface sites in the mixed system, with a lower monolayer number density of DPPC molecules being observed in the presence of dodecyl sulfate anions at the interface. Spectroscopic results also indicate that fewer dodecyl sulfate chains reside at the interface when the insoluble DPPC film is present. Increased conformational ordering of the acyl chains of both the DPPC molecules and the interfacial dodecyl sulfate anions is observed in the mixed system. Additionally, charged surfactant SDS promotes the alignment of the interfacial water molecules even in the presence of a DPPC monolayer.

Introduction

For several years, it has been recognized that organic surfactant-like molecules may play an important role in the chemistry of atmospheric aerosols.^{1–3} These surfactant species are long-chain hydrocarbons attached to various functional groups, including sulfates, phosphates, alcohols, and carboxylic acids, among others. Insoluble long-chain hydrocarbons with polar headgroups form films at the surface of aqueous aerosols in an inverse micelle configuration in which the polar headgroups associate with the aqueous subphase and the nonpolar hydrocarbon tails are oriented toward the gaseous atmosphere.^{1,2} Such surfactant films may have important effects on atmospheric processes, such as the uptake of species from the atmosphere and the evaporation of water from the aqueous aerosol core.^{1–9} In addition to the insoluble species, surfactants of a more hydrophilic nature, such as oxidized organic compounds and shorter-chain hydrocarbons, likely exist both in the aqueous core and at the surface of atmospheric aerosols. The possibility for various surfactants to compete for surface sites at the aerosol air–aqueous interface has been postulated previously.¹⁰ Because of the wide variety of organic surfactants that are believed to exist in atmospheric aerosols, a fundamental understanding of the interactions of various surfactant species at aqueous surfaces is necessary to understand the processing of such aerosols in the atmosphere.

The following is a vibrational sum frequency generation (VSFG) spectroscopy study of the interactions of a soluble organic surfactant and an insoluble lipid film at the air–aqueous interface. The soluble organic surfactant used in this study is sodium dodecyl sulfate (SDS). The insoluble surfactant film found at the aerosol surface is modeled using a dipalmitoylphosphatidylcholine (DPPC) monolayer spread at the air–water interface. Because DPPC monolayers serve as useful models for biological membranes¹¹ and SDS can be used as a model for soluble

amphiphilic biomolecules, these experiments are also applicable to studies of the interactions of biological surfactants and membranes.

Experimental Section

VSFG Theory. Detailed theoretical descriptions of the sum frequency process are available in the literature.^{12–17} Only a brief description of this technique is presented here. VSFG is a second-order nonlinear optical technique that provides vibrational spectra of interfacial molecules. In VSFG, the sum frequency beam is generated by spatially and temporally overlapping a visible beam with an infrared beam at a sample surface. The resulting sum frequency beam has a frequency, ω_{SFG} , that is the sum of the frequencies of the two incident beams, ω_{VIS} and ω_{IR} (eq 1).

$$\omega_{\text{SFG}} = \omega_{\text{VIS}} + \omega_{\text{IR}} \quad (1)$$

The detected sum frequency signal originates from the molecules residing at the interface between two isotropic bulk phases and provides molecular-level structural information of these molecules. Polarization analysis of the sum frequency signal aids in spectral interpretation.

The intensity of the sum frequency signal is shown in eq 2.

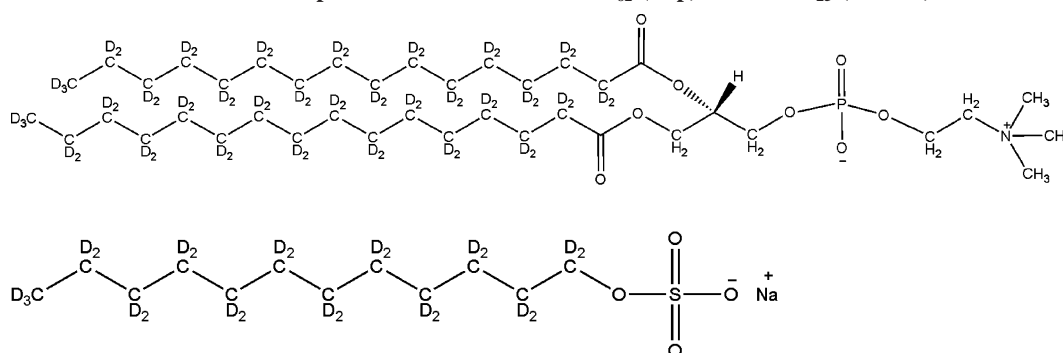
$$I^{\omega_{\text{SFG}}}(\omega) \propto |E^{\omega_{\text{SFG}}} \cdot \chi^{(2)} : E^{\omega_{\text{VIS}}} E^{\omega_{\text{IR}}}|^2 I^{\omega_{\text{VIS}}} I^{\omega_{\text{IR}}} \quad (2)$$

$I^{\omega_{\text{SFG}}}$, $I^{\omega_{\text{VIS}}}$, and $I^{\omega_{\text{IR}}}$ are the intensities of the sum frequency, incident visible, and incident infrared beams, respectively, $\chi^{(2)}$ is the macroscopic second-order nonlinear susceptibility tensor for the interfacial molecules, and the absolute square term is the electric field at the interface, where the indicated E terms include Fresnel factors that describe the relationship between the induced nonlinear polarization of the interface and both the incoming beams and the generated sum frequency beam. Detailed mathematical representations of the Fresnel factors can be found in the literature.^{13,16,18,19}

* Corresponding author. E-mail: allen@chemistry.ohio-state.edu.

- (1) Gill, P. S.; Graedel, T. E.; Weschler, C. J. *Rev. Geophys. Space Phys.* **1983**, *21*, 903.
- (2) Ellison, G. B.; Tuck, A. F.; Vaida, V. J. *Geophys. Res.* **1999**, *104*, 11633.
- (3) Donaldson, D. J.; Vaida, V. *Chem. Rev.* **2006**, *106*, 1445.
- (4) Rideal, E. K. *J. Phys. Chem.* **1925**, *29*, 1585.
- (5) Langmuir, I.; Schaefer, V. J. *J. Franklin Inst.* **1943**, *235*, 119.
- (6) Barnes, G. T. *Colloids Surf., A* **1997**, *126*, 149.
- (7) Borden, M. A.; Longo, M. L. *J. Phys. Chem. B* **2004**, *108*, 6009.
- (8) Viecelli, J.; Ma, O. L.; Tobias, D. J. *J. Phys. Chem. A* **2004**, *108*, 5806.
- (9) Gilman, J. B.; Vaida, V. *J. Phys. Chem. A* **2006**, *110*, 7581.
- (10) Gilman, J. B.; Eliason, T. L.; Fast, A.; Vaida, V. *J. Colloid Interface Sci.* **2004**, *280*, 234.

- (11) Gennis, R. B. *Biomembranes: Molecular Structure and Function*; Springer-Verlag: New York, 1989.
- (12) Shen, Y. R. *The Principles of Nonlinear Optics*; Wiley: New York, 1984.
- (13) Zhuang, X.; Miranda, P. B.; Kim, D.; Shen, Y. R. *Phys. Rev. B: Condens. Matter Mater. Phys.* **1999**, *59*, 12632.
- (14) Hirose, C.; Akamatsu, N.; Domen, K. *J. Chem. Phys.* **1992**, *96*, 997.
- (15) Moad, A. J.; Simpson, G. J. *J. Phys. Chem. B* **2004**, *108*, 3548.
- (16) Lambert, A. G.; Davies, P. B.; Neivandt, D. J. *Appl. Spectrosc. Rev.* **2005**, *40*, 103.
- (17) Gopalakrishnan, S.; Jungwirth, P.; Tobias, D. J.; Allen, H. C. *J. Phys. Chem. B* **2005**, *109*, 8861.
- (18) Hirose, C.; Akamatsu, N.; Domen, K. *Appl. Spectrosc.* **1992**, *46*, 1051.
- (19) Gopalakrishnan, S.; Liu, D.; Allen, H. C.; Kuo, M.; Shultz, M. J. *Chem. Rev.* **2006**, *106*, 1155.

Scheme 1. Simplified Structures of DPPC-*d*₆₂ (Top) and SDS-*d*₂₅ (Bottom)

$\chi^{(2)}$ is composed of a nonresonant term and a sum of resonant terms (eq 3).

$$|\chi^{(2)}|^2 = |\chi_{\text{NR}}^{(2)} + \sum_v \chi_v^{(2)}|^2 \quad (3)$$

$\chi_v^{(2)}$, the macroscopic nonlinear susceptibility for a vibration v , is related to the molecular hyperpolarizability for that vibration, as shown in eq 4.

$$\chi_v^{(2)} = N \sum_{lmn} \langle \mu_{IJK:lmn} \rangle \beta_v \quad (4)$$

N represents the number density of the surface species, β_v represents the molecular hyperpolarizability for the v vibrational mode, $\mu_{IJK:lmn}$ represents an Euler angle transformation between the laboratory reference frame (denoted by subscripts I, J , and K) and the molecular reference frame (denoted by subscripts l, m , and n), and $\langle \cdots \rangle$ represents an average over the orientational distribution of the molecules. The representation of the molecular hyperpolarizability in the molecular reference frame is given in eq 5.

$$\beta_{lmn,v} = \frac{\langle g | \alpha_{lm} | v \rangle \langle v | \mu_n | g \rangle}{\omega_{\text{IR}} - \omega_v + i\Gamma_v} \quad (5)$$

ω_v is the frequency of the vibrational transition, Γ is the natural line width of the transition, $\langle g | \alpha_{lm} | v \rangle$ is the Raman transition moment, and $\langle v | \mu_n | g \rangle$ is the infrared transition moment where g is the ground vibrational state and v is the excited vibrational state. When the frequency of the incident infrared beam approaches the frequency of the vibrational transition, $\omega_{\text{IR}} - \omega_v$ approaches zero, and the value of $\chi_v^{(2)}$ increases, resulting in an increase in the intensity of the sum frequency signal. Furthermore, the molecular hyperpolarizability is nonzero only when the Raman and infrared transition moments are nonzero. Thus, a vibrational mode must be both Raman- and infrared-active in order for it to be SFG-active. Symmetry constraints arising from this selection rule lead to the requirement for a lack of inversion symmetry for sum frequency generation to be allowed. Macroscopically, this requirement is fulfilled at interfaces between two isotropic bulk phases. Sum frequency generation is forbidden in bulk phases where the molecules experience a centrosymmetric environment. The molecules residing at the interface between two isotropic bulk phases experience a noncentrosymmetric environment and are SFG-active by this selection rule. Furthermore, a bilayer exhibiting perfect inversion symmetry would be SFG-inactive, whereas sum frequency signal would result from a monolayer or trilayer.

Instrumentation. The broad bandwidth sum frequency generation (BBSFG) spectrometer^{20,21} employed in these experiments uses two regenerative amplifiers (Spectra-Physics Spitfire, femtosecond and picosecond versions) to produce femtosecond and picosecond visible pulsed laser beams with 1 kHz repetition rates. Each regenerative

amplifier is seeded by half of the output from a mode-locked Ti:sapphire laser (Spectra-Physics Tsunami) and is pumped by a Q-switched all-solid-state Nd:YLF laser (Spectra-Physics Evolution-30). The output of the femtosecond regenerative amplifier (800 nm center wavelength, $\sim 300 \text{ cm}^{-1}$ bandwidth, 85 fs pulse duration)²⁰ is used in an optical parametric amplifier (OPA, Spectra-Physics OPA-800CF) to generate broad bandwidth infrared pulses ($> 300 \text{ cm}^{-1}$ in both the C–H and C–D stretching regions). The wavelength region of the infrared output is selected by angle tuning a β -barium borate crystal in the OPA. The broad bandwidth infrared beam is spatially and temporally overlapped at the sample surface with the output of the picosecond regenerative amplifier (800 nm center wavelength, 15 cm^{-1} bandwidth, 2 ps pulse duration)²⁰ to generate the broad bandwidth sum frequency beam ($> 300 \text{ cm}^{-1}$ in both the C–H and C–D stretching regions). A co-propagating geometry is used for the visible and infrared beams, and the reflected sum frequency beam is detected. In the following experiments, the input energy of the visible beam is $300 \mu\text{J}$, and the input energy of the infrared beam is $5 \mu\text{J}$ in the C–D region and $6 \mu\text{J}$ in the C–H region. The angles of the infrared, visible, and sum frequency beams from the surface normal are 69, 58, and 60°, respectively.

The reflected visible beam is spatially filtered after the sample, and all residual light is optically filtered by two short-pass (SPF-750, CVI, Albuquerque, NM) and two notch (Kaiser Optical Systems, Inc., Ann Arbor, MI) filters positioned in the sum frequency beam line. The sum frequency beam is dispersed by a 1200 g/mm grating blazed at 750 nm in a 500 mm monochromator (Acton Research, SpectraPro SP-500) and then detected by a liquid-nitrogen-cooled CCD (Roper Scientific, LN 400EB, back-illuminated, 1340×400 pixel array). The monochromator is controlled using SpectraSense software (Acton Research, version 4.4.0).

Sum frequency peak positions are calibrated in the C–H stretching region using the absorption bands of a polystyrene film positioned in the infrared beam line during the acquisition of a sum frequency spectrum of a GaAs crystal. In the C–D stretching region, sum frequency peak positions are calibrated using the absorption bands of ambient CO_2 vapor. Background spectra are acquired for each sample by disrupting the temporal overlap of the beams, and the background-subtracted sum frequency spectra are normalized to the nonresonant signal from a GaAs crystal surface. Polarization selection is achieved using a MgF_2 window in the infrared beam, a half-wave plate in the visible beam, and a Glan polarizer in the sum frequency beam. The resolution of the BBSFG system is approximately 8 cm^{-1} .²²

Materials. 1,2-Dipalmitoyl-*sn*-glycero-3-phosphocholine (DPPC) and 1,2-dipalmitoyl-*sn*-glycero-3-phosphocholine-*d*₆₂ (DPPC-*d*₆₂) were obtained from Avanti Polar Lipids, Inc. (Alabaster, AL). Sodium dodecyl sulfate (SDS, 99+%, ACS reagent grade) and chloroform ($\geq 99.8\%$, ACS spectrophotometric grade) were obtained from Sigma-Aldrich. Sodium dodecyl sulfate-*d*₂₅ (SDS-*d*₂₅, 98%) was obtained from Cambridge Isotope Laboratories, Inc. (Andover, MA). All chemicals were used as received. Deionized water was obtained from a Barnstead Nanopure filtration system with a minimum resistivity of $18.2 \text{ M}\Omega \text{ cm}$.

(20) Hommel, E. L.; Ma, G.; Allen, H. C. *Anal. Sci.* **2001**, *17*, 1325.

(21) Ma, G.; Allen, H. C. *J. Phys. Chem. B* **2003**, *107*, 6343.

(22) Ma, G.; Allen, H. C. *Photochem. Photobiol.* **2006**, *82*, 1517.

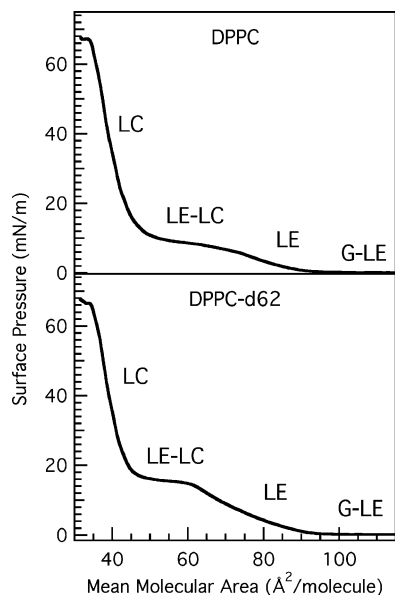


Figure 1. Surface pressure–area compression isotherms of DPPC (top) and DPPC- d_{62} (bottom) with phases labeled: G, gas; LE, liquid-expanded; and LC, liquid-condensed. G-LE and LE-LC are areas of coexistence of the specified phases.

Method. Experiments were performed to separately investigate the insoluble lipid film, DPPC or DPPC- d_{62} , and the soluble surfactant, SDS or SDS- d_{25} . Simplified structures of the deuterated species, DPPC- d_{62} and SDS- d_{25} , are shown in Scheme 1. To study the insoluble film, 12.0 μL of the lipid of interest (~ 1 mM DPPC or DPPC- d_{62} in chloroform) was spread on 20 mL of water in a Petri dish (5 cm diameter) using a 50 μL Hamilton syringe. The resulting film (lipid monolayer in equilibrium with its bulk liquid phase) had an initial surface pressure of 48 mN/m before solvent evaporation.

After waiting 10 min to ensure the complete evaporation of chloroform and spreading of the lipid, we obtained VSFG spectra of the lipid monolayer at the air–water interface in relevant polarization combinations. SSP (S-polarized sum frequency, S-polarized visible, P-polarized infrared), SPS (S-polarized sum frequency, P-polarized visible, S-polarized infrared), and PPP (P-polarized sum frequency, P-polarized visible, P-polarized infrared) polarization combinations are used for these experiments. The electric field is perpendicular to the plane of incidence for S-polarized light and is parallel to the plane of incidence for P-polarized light. Upon evaporation of the solvent, the surface pressure dropped by a few mN/m and continued to drop slowly over time. The spectroscopic measurements were obtained while the phospholipid monolayer was in the liquid-condensed phase. The phases of the lipid monolayer are labeled on the surface pressure–area compression isotherms of DPPC and DPPC- d_{62} shown in Figure 1. The phases represented on the isotherms are characteristic of these phospholipids^{23–26} and follow the labeling conventions reported elsewhere in the literature.^{26,27}

Concentrated SDS or SDS- d_{25} solution (~ 17 mM in water) was injected into the water subphase using a 1 mL Hamilton syringe to form a 2 mM SDS subphase. To prevent disruption of the lipid monolayer during the injection process, the Petri dish had a small glass tube (~ 0.3 cm diameter half-cylinder) attached vertically to its inner wall. The lower edge of the tube is approximately 0.5 cm above the bottom of the dish, and the upper edge of the tube is approximately 1 cm above the upper rim of the dish. The tube provides direct access to the subphase without requiring the needle to penetrate the lipid monolayer at the air–water interface. After the injection

of SDS or SDS- d_{25} , the VSFG signal of the lipid was monitored in the SSP polarization combination until stability was observed. After the stabilization of the signal, VSFG spectra were recorded in relevant polarization combinations SSP, SPS, and PPP. The VSFG spectra of the lipid monolayer on the two subphases were compared.

Unlike the experiments used to probe the lipid molecules, in which the same sample was probed both before and after injection of SDS (or SDS- d_{25}) into the subphase, the experiments used to probe the interfacial deuterated dodecyl sulfate chains compare two separate samples. In the first sample, concentrated SDS- d_{25} was injected into 20 mL of water in a Petri dish to form a 2 mM SDS- d_{25} solution in the absence of the lipid monolayer. The second sample differs from the first sample only in that the lipid monolayer was present at the air–aqueous interface. For both samples, the VSFG signal (SSP polarization combination) from the deuterated dodecyl sulfate anions at the interface was monitored after injection until stability was achieved. Spectra were then obtained in relevant polarization combinations SSP, SPS, and PPP and compared for the two systems.

All reported spectra are the average of up to three 2-min acquisitions and are normalized to the nonresonant VSFG signal from a GaAs crystal surface. It should be noted that the reported experimental observations are for a nonequilibrium system. Because processes unrelated to the interactions between the DPPC and SDS molecules become important on longer time scales, a long-term (> 4 h) state of equilibrium, defined by spectral stability, was not obtainable. Nonetheless, the reported VSFG spectra showed stability and were reproducible for the acquisition period. However, significant and continuous changes in the spectra were observed over longer periods of time. Because of the variety of processes that might occur on long time scales (such as evaporation, adsorption of the surfactants to the glass dish, solubilization of the lipid, etc.),^{28,29} only the initial spectral changes can be clearly interpreted as originating from the interactions between SDS and DPPC, as reported herein. Peak frequencies are reported as the observed frequencies, not from spectral fits.

Results and Discussion

To determine how soluble surfactant SDS- d_{25} affects the molecules of a DPPC Langmuir monolayer at the air–aqueous interface, VSFG SSP spectra of a DPPC monolayer were obtained in the C–H stretching region both before and after injection of concentrated SDS- d_{25} into the water subphase and are shown in Figure 2a. Because the SDS- d_{25} molecules are fully deuterated, the VSFG signal originates solely from the DPPC molecules at the air–aqueous interface. VSFG spectra for all polarization combinations of the DPPC monolayer on water and SDS- d_{25} subphases are shown in Figure 2a–c.

The observed peaks in Figure 2 have contributions from the vibrational resonances of both the acyl chains and the phosphocholine headgroups of the DPPC molecules. In the SSP spectrum of the DPPC monolayer on a water subphase (Figure 2a, black spectrum), the small peak at 2840 cm^{-1} is assigned to the CH_2 symmetric stretch (SS) of the acyl chains, the peak at 2872 cm^{-1} is assigned to the CH_3 SS of the acyl chains, the shoulder at 2905 cm^{-1} is assigned to the CH_2 Fermi resonance (FR) of the acyl chains with a contribution from the CH_2 SS of the phosphocholine headgroups, and the peak at 2946 cm^{-1} has contributions from the CH_3 FR and CH_3 asymmetric stretch (AS) of the acyl chains and the CH_2 AS and CH_3 SS of the phosphocholine headgroups. In the spectrum of the DPPC monolayer on a 2 mM SDS- d_{25} subphase (Figure 2a, red spectrum), the peak at 2876 cm^{-1} is assigned to the CH_3 SS of the acyl chains, the shoulder at 2905 cm^{-1} is assigned to the CH_2

(23) Kane, S. A.; Compton, M.; Wilder, N. *Langmuir* **2000**, *16*, 8447.

(24) Roke, S.; Schins, J.; Muller, M.; Bonn, M. *Phys. Rev. Lett.* **2003**, *90*, 128101/1.

(25) McConlogue, C. W.; Malamud, D.; Vanderlick, T. K. *Biochim. Biophys. Acta Biomembr.* **1998**, *1372*, 124.

(26) Ma, G.; Allen, H. C. *Langmuir* **2006**, *22*, 5341.

(27) Kaganer, V. M.; Mohwald, H.; Dutta, P. *Rev. Mod. Phys.* **1999**, *71*, 779.

(28) Gaines, G. L., Jr. *Insoluble Monolayers at Liquid-Gas Interfaces*; Interscience Publishers: New York, 1966.

(29) Adamson, A. W.; Gast, A. P. *Physical Chemistry of Surfaces*, 6th ed.; John Wiley & Sons: New York, 1997.

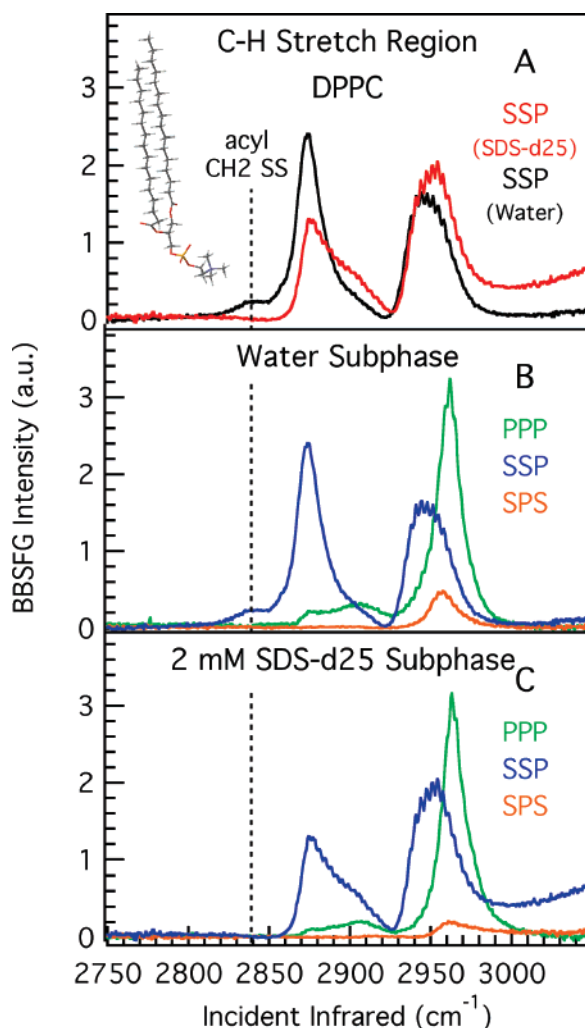


Figure 2. VSFG spectra probing DPPC molecules in the C–H stretching region. (A) SSP polarization combination: water subphase (black) and 2 mM SDS- d_{25} subphase (red). (B) Water subphase: SSP (blue), PPP (green), and SPS (orange). (C) 2 mM SDS- d_{25} subphase: SSP (blue), PPP (green), and SPS (orange).

FR of the acyl chains with contribution from the CH_2 SS of the phosphocholine headgroups, and the peak at 2952 cm^{-1} has contributions from the CH_3 FR and CH_3 AS of the acyl chains and the CH_2 AS and CH_3 SS of the phosphocholine headgroups. Acyl chain assignments are from Liu and Conboy,³⁰ and headgroup assignments are from Conboy.³¹ The polarization data in Figure 2b,c are useful for spectral interpretation. For example, Lu and co-workers³² developed polarization selection rules using molecular symmetry arguments that provide verification of the above assignments when used in conjunction with the experimental VSFG polarization data.

Each acyl chain in a DPPC molecule has an even number (14) of CH_2 groups. For an all-trans configuration, adjacent methylene groups are in an anti conformation with all C–C bonds of the chain residing in the same plane. For such a configuration, local inversion symmetry exists between adjacent pairs of methylene groups in the acyl chains. The SS resonances of the CH_2 groups are not SFG-active for an all-trans configuration because a lack of inversion symmetry is required for sum frequency activity.^{26,33} The presence of a peak corresponding to the SS vibrations of the

acyl chain CH_2 groups is a signature of conformational disorder in the chains. In Figure 2a, a peak assigned to the CH_2 SS of the acyl chains is present in the spectrum corresponding to the water subphase and is absent in the spectrum corresponding to the SDS- d_{25} subphase, indicating that the DPPC molecules are more conformationally ordered (i.e., have fewer gauche defects) in the presence of SDS- d_{25} . This result is consistent with the observation by Meister and co-workers of a small increase in the order of the acyl chains of DMPC- d_{54} molecules upon incorporation of SDS into a DMPC- d_{54} monolayer using reflection–absorption infrared spectroscopy (RAIRS).³⁴

The increased VSFG intensity from 2975 to 3050 cm^{-1} in the spectrum corresponding to the SDS- d_{25} subphase compared to that corresponding to the water subphase is assigned to aligned interfacial water molecules. The electrostatic field created at the interface by the charge on the sulfate headgroups of the deuterated dodecyl sulfate anions promotes increased alignment of the water molecules at the interface.³⁵

Additional differences exist between the spectra in Figure 2a, but the multitude of vibrational resonances contributing to the observed peaks makes interpretation difficult. Although the analysis of additional polarization combinations SPS and PPP are helpful in deciphering vibrational assignments,³² these spectra do not allow the complete deconvolution of the overlapping spectral resonances. Therefore, to separately determine the effects of SDS- d_{25} on the acyl chains and the phosphocholine headgroups of the lipid molecules, experiments using various combinations of DPPC- d_{62} , SDS, and SDS- d_{25} in the C–H and C–D stretching regions were performed. The interfacial deuterated dodecyl sulfate anions were also investigated in the C–D stretching region in the presence and absence of a DPPC monolayer.

The vibrational resonances exclusively from the lipid headgroup are selectively probed in the C–H stretching region using a DPPC- d_{62} monolayer on both water and 2 mM SDS- d_{25} subphases, and the resulting spectra are shown in Figure 3. Because DPPC- d_{62} molecules have deuterated acyl chains and non-deuterated headgroups (refer to Scheme 1), only the vibrational resonances of the DPPC- d_{62} headgroups are probed in these experiments. Figure 3a shows the VSFG spectra, SSP polarization combination, of the lipid monolayer both before (black spectrum) and after (red spectrum) injection of the concentrated SDS- d_{25} solution into the water subphase. VSFG spectra of the lipid headgroup on water and SDS- d_{25} subphases in all polarization combinations were obtained (Figure 3b,c) but are of insufficient signal/noise to provide insight beyond qualitative clarification of the spectral assignments.

Following the spectral assignments for the phosphocholine headgroup proposed by Conboy and co-workers,^{30,31} peaks corresponding to the CH_2 SS (2909 cm^{-1}), the CH_2 AS (low-frequency side of the 2956 cm^{-1} peak), and the CH_3 SS (high-frequency side of the 2956 cm^{-1} peak) are present in the SSP spectra (Figure 3a) both before and after injection of SDS- d_{25} into the subphase. In the spectrum of the DPPC- d_{62} headgroups on the SDS- d_{25} subphase (red spectrum), a broad VSFG intensity that increases with increasing wavenumber is assigned to the aligned interfacial water molecules caused by the charge of the deuterated dodecyl sulfate anions.³⁵ This broad intensity contributes to the enhancement of the observed DPPC- d_{62} headgroup peaks in the spectrum corresponding to the SDS- d_{25} subphase compared to those for the water subphase. The enhanced

(30) Liu, J.; Conboy, J. C. *Langmuir* **2005**, *21*, 9091.

(31) Conboy, J. C. Personal communication, 2007.

(32) Lu, R.; Gan, W.; Wu, B. h.; Zhang, Z.; Guo, Y.; Wang, H.-f. *J. Phys. Chem. B* **2005**, *109*, 14118.

(33) Guyot-Sionnest, P.; Hunt, J. H.; Shen, Y. R. *Phys. Rev. Lett.* **1987**, *59*, 1597.

(34) Meister, A.; Kerth, A.; Blume, A. *J. Phys. Chem. B* **2004**, *108*, 8371.

(35) Gragson, D. E.; McCarty, B. M.; Richmond, G. L. *J. Am. Chem. Soc.* **1997**, *119*, 6144.

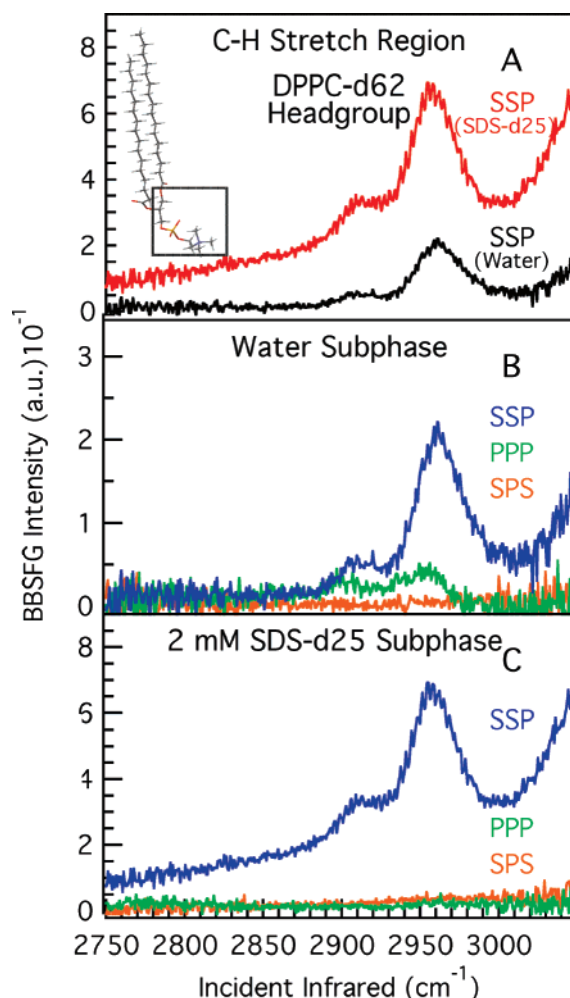


Figure 3. VSFG spectra probing the headgroups of DPPC- d_{62} in the C-H stretching region. (A) SSP polarization combination: water subphase (black) and 2 mM SDS- d_{25} subphase (red). (B) Water subphase: SSP (blue), PPP (green), and SPS (orange). (C) 2 mM SDS- d_{25} subphase: SSP (blue), PPP (green), and SPS (orange).

interfacial water signal in the presence of soluble surfactant SDS- d_{25} is direct spectral evidence that SDS- d_{25} affects the air-aqueous interface even in the presence of a DPPC- d_{62} Langmuir monolayer.

The acyl chains of the lipid molecules are studied using a DPPC- d_{62} monolayer on both water and 2 mM SDS subphases in the C-D stretching region, and the resulting spectra are shown in Figure 4. Because the lipid headgroups are not deuterated in the DPPC- d_{62} molecules, only the vibrational resonances of the acyl chains are selectively probed in these experiments. In the SSP spectrum of the DPPC- d_{62} monolayer on water (Figure 4a, black spectrum), the peaks present correspond to the CD_3 SS (2070 cm^{-1}), CD_3 FR (2125 cm^{-1}), and CD_3 AS (2218 cm^{-1}) of the acyl chains of DPPC- d_{62} .^{22,36} The same vibrational resonances contribute to the peaks observed in the SSP spectrum of the monolayer on 2 mM SDS (Figure 4a, red spectrum).

The absence of VSFG intensity in the region corresponding to the CD_2 SS (approximately 2100 cm^{-1})³⁶ in both spectra shown in Figure 4a suggests that the lipid molecules are conformationally ordered in an all-trans configuration on both the water and SDS subphases. However, this conclusion appears to be in direct conflict with the results of Figure 2a, where a peak assigned to the CH_2 SS of the acyl chains is readily observed for DPPC

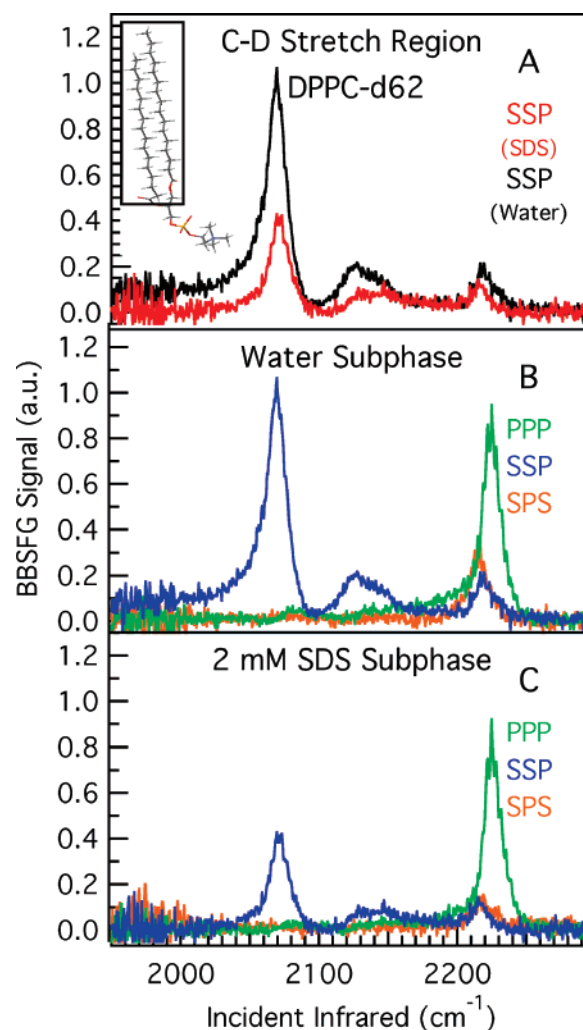


Figure 4. VSFG spectra probing the acyl chains of DPPC- d_{62} in the C-D stretching region. (A) SSP polarization combination: water subphase (black) and 2 mM SDS subphase (red). (B) Water subphase: SSP (blue), PPP (green), and SPS (orange). (C) 2 mM SDS subphase: SSP (blue), PPP (green), and SPS (orange).

molecules on a water subphase. The presence of a CH_2 SS peak indicates that gauche defects are present in the acyl chains of the DPPC molecules on a water subphase. This inconsistency is possibly explained by a reduction in oscillator strength for deuterated methylene stretching modes compared to that for non-deuterated methylene stretching modes, which translates to improved detection limits for gauche defects in the acyl chains of the non-deuterated DPPC monolayer. Therefore, on the basis of Figure 2a, DPPC molecules possess a detectable fraction of gauche defects in the monolayer on water.

In Figure 4a, the CD_3 SS peak in the spectrum corresponding to the lipid monolayer on the SDS subphase (red spectrum) has a lower intensity than in the spectrum corresponding to the water subphase (black spectrum). Because sum frequency intensity is a function of both number density and orientational order, the decrease in intensity of the CD_3 SS peak observed upon injection of SDS into the subphase must be a result of either a decrease in the number density of lipid molecules in the monolayer at the interface or a change in the orientation of the terminal methyl groups of the DPPC- d_{62} acyl chains.

As explained in detail by Ma and Allen,²⁶ the average angle of the C_3 axis of the terminal methyl groups of the DPPC- d_{62} acyl chains from the surface normal can be estimated using the ratio of eqs 6 and 7 below.³⁷

(36) Yang, C. S. C.; Richter, L. J.; Stephenson, J. C.; Briggman, K. A. *Langmuir* 2002, 18, 7549.

$$\chi_{\text{SSP}}^{(2)}(\text{CD}_3\text{SS}) = \frac{1}{2}N\beta_{\text{ccc}}[\cos\theta(1+r) - \cos^3\theta(1-r)] \quad (6)$$

$$\chi_{\text{SSP}}^{(2)}(\text{CD}_3\text{AS}) = -N\beta_{\text{caa}}[\cos\theta - \cos^3\theta] \quad (7)$$

$\chi_{\text{SSP}}^{(2)}(\nu)$ is the macroscopic second-order nonlinear susceptibility of the specified vibration ν in the SSP polarization combination, N is the number density of interfacial molecules, β_{lmn} is the specified molecular hyperpolarizability, θ is the average orientation angle of the C_3 axis of the terminal methyl groups from the surface normal, and r is the ratio $(\beta_{\text{aac}})/(\beta_{\text{ccc}})$. Here, r is equal to 2.3³⁷ and $(\beta_{\text{caa}})/(\beta_{\text{aac}})$ is equal to 4.2.^{38,39} The ratio of the susceptibilities of the CD_3 SS to the CD_3 AS is estimated experimentally by taking the square root of the ratio of the experimental VSFG intensities (component peak areas from spectral fits) of the CD_3 SS peak to the CD_3 AS peak. Using this method, θ is calculated to be $16.6 \pm 0.6^\circ$ for DPPC- d_{62} on water and $17.0 \pm 0.6^\circ$ for DPPC- d_{62} on 2 mM SDS. The small difference in θ calculated for the two subphases is well within the error of the calculation. Therefore, the average angle of the C_3 axis of the terminal methyl groups from the surface normal is virtually the same for the DPPC- d_{62} molecules on water and SDS subphases.

Because the angle between the C_3 axis of the terminal methyl group and the axis of the acyl chain is fixed for an all-trans chain configuration, a change in the tilt angle of the chains from the surface normal accompanies a change in θ . Assuming that the number of gauche defects in the lipid molecules is small for the water subphase and negligible for the SDS subphase, equivalent θ values for the DPPC- d_{62} molecules on the two subphases translates to equivalent chain tilt angles for the DPPC- d_{62} molecules on the two subphases. Because a significant change in the orientation of the DPPC molecules on the two subphases is not observed, the decrease in VSFG intensity for the DPPC- d_{62} monolayer on the 2 mM SDS subphase compared to the water subphase is attributed to a decrease in the monolayer number density of DPPC- d_{62} molecules at the interface. The formation of aggregate structures of DPPC- d_{62} in the presence of SDS cannot be discounted because any inversion symmetry associated with 3D aggregates would appear spectroscopically as a decrease in monolayer number density based on the selection rules for VSFG. Previous studies using Brewster angle microscopy and fluorescence microscopy have shown that the penetration of soluble surfactants into insoluble monolayers can affect the aggregation properties (including the sizes and shapes of domains) and phase transitions of the insoluble film at the interface.^{25,40,41} Furthermore, the RAIRS studies by Meister et al. indicated that the incorporation of SDS molecules into the insoluble phospholipid (DMPC- d_{54}) film did not significantly affect the number density of the phospholipid at the surface.³⁴ A consideration of the different selection rules for the infrared surface study (specifically, the fact that the infrared technique has a finite probe depth and does not necessarily probe only a monolayer) provides support for the possibility of the formation of 3D aggregates of the lipid molecules in the presence of soluble surfactant SDS.

In addition to probing the lipid molecules in this mixed system, soluble surfactant SDS- d_{25} was also probed in the C–D stretching

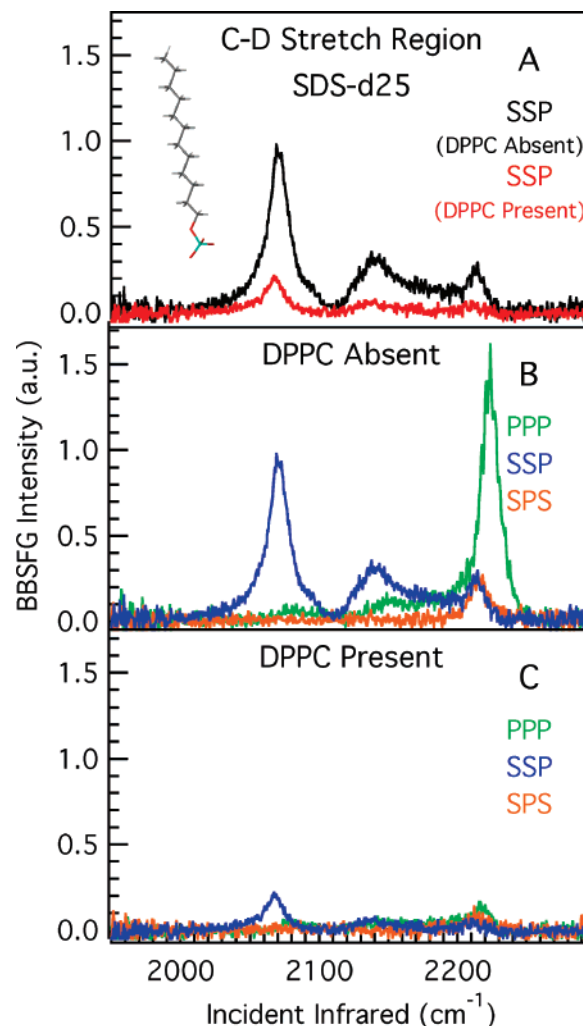


Figure 5. VSFG spectra probing the SDS- d_{25} chains in the C–D stretching region. (A) SSP polarization combination: in the absence (black) and presence (red) of the DPPC monolayer. (B) In the absence of the DPPC monolayer: SSP (blue), PPP (green), and SPS (orange). (C) In the presence of the DPPC monolayer: SSP (blue), PPP (green), and SPS (orange).

region in both the presence and absence of a DPPC monolayer, and the resulting VSFG spectra are shown in Figure 5. Because sum frequency generation is an interface-selective spectroscopic technique, only the deuterated dodecyl sulfate chains at the air–aqueous interface contribute to the VSFG signal in these experiments. Additional changes to those described below have been observed to occur in the spectra over a longer period of time. As noted previously, several additional processes that might become important on longer time scales (evaporation, adsorption of the surfactants to the glass dish, solubilization of the lipid, etc.)^{28,29} make the interpretation complex and are beyond the scope of this discussion.

In the VSFG SSP spectrum of the SDS- d_{25} chains in the absence of a DPPC monolayer, shown in Figure 5a (black spectrum), the peak at 2070 cm^{-1} is assigned to the CD_3 SS with the shoulder at 2095 cm^{-1} assigned to the CD_2 SS, the peak at 2140 cm^{-1} is assigned to the CD_3 FR with some contribution from the CD_2 FR, and the peak at 2212 cm^{-1} is assigned to the CD_3 AS.³⁶ The CD_2 FR and CD_2 AS of the interfacial SDS- d_{25} chains may contribute to the observed intensity in the $2150\text{--}2200\text{ cm}^{-1}$ region.³⁶ The presence of peaks assigned to SS resonances of the CD_2 groups indicates that the SDS- d_{25} chains possess some gauche defects and are not completely ordered at the interface. This

(37) Zhang, D.; Gutow, J.; Eiseenthal, K. B. *J. Phys. Chem.* **1994**, *98*, 13729.

(38) Watanabe, N.; Yamamoto, H.; Wada, A.; Domen, K.; Hirose, C.; Ohtake, T.; Mino, N. *Spectrochim. Acta, Part A* **1994**, *50A*, 1529.

(39) Wang, C.-Y.; Groenzin, H.; Shultz, M. J. *J. Phys. Chem. B* **2004**, *108*, 265.

(40) Fainerman, V. B.; Zhao, J.; Vollhardt, D.; Makievski, A. V.; Li, J. B. *J. Phys. Chem. B* **1999**, *103*, 8998.

(41) Vollhardt, D.; Fainerman, V. B. *Adv. Colloid Interface Sci.* **2000**, *86*, 103.

result is in agreement with previous studies of SDS at the air–aqueous interface that report conformational disorder in the interfacial SDS chains even at maximum surface coverage.^{34,42,43}

Although the VSFG signal from the SDS-*d*₂₅ chains appears immediately after injection in the absence of a DPPC monolayer, the signal first appears approximately 30 min after injection in the presence of a DPPC monolayer. This indicates either a low number density of interfacial SDS-*d*₂₅, a large degree of disorder in the interfacial SDS-*d*₂₅, or a combination of these two phenomena occurring at the interface immediately after the injection of SDS-*d*₂₅ in the presence of a DPPC monolayer. Because a phosphocholine headgroup occupies approximately 45 Å² at the surface,²⁷ the initial space available for SDS-*d*₂₅ at the liquid surface is limited. Over time, the SDS-*d*₂₅ anions compete with the DPPC surface molecules and incorporate into the lipid monolayer, and VSFG signal is observed. Previous studies also provide evidence for the incorporation of SDS into a lipid monolayer in the liquid-condensed phase. For example, Meister et al. report a surface pressure increase over time upon injection of SDS into the subphase of a DMPC-*d*₅₄ monolayer in the liquid-condensed phase.³⁴

In Figure 5a, the red spectrum corresponds to interfacial SDS-*d*₂₅ in the presence of a DPPC monolayer after temporary stability of the signal is achieved. This spectrum has similar features to the spectrum corresponding to the absence of DPPC (Figure 5a, black spectrum) but has a much lower intensity. The spectrum of the SDS-*d*₂₅ chains corresponding to the absence of DPPC (black spectrum) shows significant asymmetry in the CD₃ SS peak due to the presence of a CD₂ SS shoulder. However, the spectrum corresponding to the presence of DPPC (red spectrum) has a more symmetric CD₃ SS peak, indicating a lower proportion of gauche defects and a slight increase in conformational order of the interfacial SDS-*d*₂₅ chains in the presence of the lipid monolayer. Again, this result is consistent with the observation by Meister et al. of a small increase in the order of SDS molecules

incorporated into a DMPC-*d*₅₄ monolayer using RAIRS.³⁴ A possible explanation for the increase in conformational order of the SDS-*d*₂₅ chains is that the presence of the lipid monolayer at the liquid surface sterically hinders the interfacial SDS-*d*₂₅ chains from adopting disordered conformations with many gauche defects. Because an increase in order is expected to increase the VSFG signal, the lower signal observed for SDS-*d*₂₅ in the presence of a DPPC monolayer compared to that observed in the absence of a DPPC monolayer is attributed to a lower number density of interfacial SDS-*d*₂₅. The presence of the DPPC monolayer limits the number of dodecyl sulfate anions that can reside at the aqueous surface. However, a reduction in the overall DPPC-*d*₆₂ monolayer spectral intensity observed for the SDS subphase in Figure 4a indicates that the soluble surfactant does, in fact, lower the monolayer number density of the lipid molecules.

Conclusions

An investigation of the interactions of a DPPC Langmuir monolayer with soluble surfactant SDS was presented. Charged surfactant SDS promotes the alignment of interfacial water molecules even in the presence of a DPPC monolayer. In addition, the soluble surfactant anions influence the conformations of the lipid molecules at the surface. In the presence of SDS, interfacial DPPC molecules are more ordered (have fewer gauche defects) and have a lower monolayer number density than when residing on a pure water subphase. The presence of the insoluble lipid monolayer at the air–aqueous interface limits the number of soluble surfactant anions that can reside at the aqueous surface and promotes increased conformational ordering of the interfacial soluble surfactant chains. These findings are evidence that soluble organic surfactants have the potential to influence the surface structure of atmospheric aerosols, which may have important implications in the atmospheric processing of such aerosols.

Acknowledgment. We thank the National Science Foundation (ATM-0413893) for funding this work.

LA7006974

(42) Prosser, A. J.; Franses, E. I. *Langmuir* **2002**, *18*, 9234.

(43) Gragson, D. E.; McCarty, B. M.; Richmond, G. L. *J. Phys. Chem.* **1996**, *100*, 14272.